한국전산구조공학회
2002년도 가을 학술발표회 논문집

직교 좌표계에 의한 정현형 수평 곡선보의 자유진동 해석

Free Vibration Analysis of Horizontally Sinusoidal Curved Beams in Cartesian Coordinates

이 병 구† · 이 태 은* · 강 희 종** · 김 권 식***

Byoung Koo Lee · Tae Eun Lee · Hee Jong Kang · Kweon Sik Kim

ABSTRACT

The differential equations governing free vibrations of the elastic, horizontally curved beams with unsymmetric axis are derived in Cartesian coordinates rather than in polar coordinates, in which the effect of torsional inertia is included. Frequencies are computed numerically for the sinusoidal curved beams with both clamped ends and both hinged ends. Comparisons of natural frequencies between this study and SAP 2000 are made to validate theories and numerical methods developed herein. The convergent efficiency is highly improved under the newly derived differential equations in Cartesian coordinates. The lowest four natural frequency parameters are reported, with and without torsional inertia, as functions of three non-dimensional system parameters: the horizontal rise to chord length ratio, the span length to chord length ratio, and the slenderness ratio.

Keywords: *Cartesian coordinates, free vibration, harmonic motion, sinusoidal curved beam, mode shape, natural frequency, torsional inertia, unsymmetric axis.*

1. Introduction

Studies on the free vibrations of linearly elastic horizontally curved beams of various shapes have been reported for more than three decades. Studies concerning with this subject was critically reviewed by Lee et al.[1]. Briefly, such works included studies of circular curved beams with predictions of the lowest frequency by Volterra and Morell[2], Romanelli and Laura[3], and Maurizi et al.[4]; studies of non-circular curved beams with predictions of higher frequencies by Irie et al.[5], Kawakami et al.[6], Kang et al.[7], Yildirim[8] and Lee et al.[9]; and studies showing the effect of rotatory inertia on free vibration frequencies by Laskey[10] and Mo[11].

This paper has three main purposes: (1) to present the differential equations for free vibrations of horizontally curved beams where all equations are derived in the Cartesian coordinates rather than in polar coordinates; (2) to include the torsional inertia in the differential equations; and (3) to illustrate the numerical solutions to the newly derived equations for a broad class of sinusoidal curved beams.

In most previous works on curved beam vibrations, the polar coordinates were employed and the effect of torsional inertia was excluded in the differential equations. The results presented herein extent significantly previous works. That is, using the Cartesian formulation together with highly efficient and convergent numerical methods, the free vibration frequencies, with and without torsional inertia, are investigated for sinusoidal curved beams with unsymmetric axis. Such numerical results are presented for both clamped ends and both hinged ends. The lowest four non-dimensional frequency parameters are shown as functions of three system parameters: the horizontal rise to chord length ratio, the span length to chord length ratio, and the slenderness ratio.

† Member, Professor, School of Civil and Environmental Engineering, Wonkwang University, Iksan, Junbuk 570-749, Korea (E-mail: bkleest@wonkwang.ac.kr)
* Member, Graduate Student, Wonkwang University
** Chungryong Construction Co. Ltd.
*** SK Engineering & Construction Co. Ltd.

The following assumptions are inherent in this theory: the curved beam is linearly elastic and the small deflection theory is governed. In addition, the curved beam is assumed to be in harmonic motion.

2. Mathematical Model

The geometry and nomenclature of the horizontally curved beam with unsymmetric axis, placed in Cartesian coordinates (x, y, v), are shown in Fig. 1. The curved beam is supported by both clamped ends or both hinged ends. The geometric variables are defined as follows.

L : Span length
l : Chord length
h : Horizontal rise
v : Vertical displacement
ψ : Rotation of cross-section
ϕ : Torsional angle of beam axis
ρ : Radius of curvature
θ : Inclination of ρ with x-axis

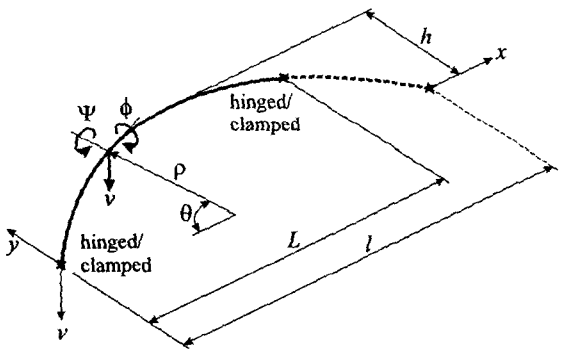

Fig. 1 Geometry of curved beam

The shape of sinusoidal curved beam, which is chosen as the object beam herein, is expressed in terms of (l, h) and the coordinate x in the range from $x = 0$ to $x = L$. That is,

$$y = h\sin(\pi x / l), \quad 0 \le x \le L \tag{1}$$

A small element of the horizontally curved beam is shown in Fig. 2 in which are defined the positive directions for the shear force Q, the bending moment M, the torsional moment T, the vertical inertia force F_v and the torsional inertia torque C_ϕ. Treating F_v and C_ϕ as equivalent static quantities, the three equations for "dynamic equilibrium" of the element are

$$Q' - \rho F_v = 0 \tag{2}$$
$$M' - \rho Q + T = 0 \tag{3}$$
$$M - T' + \rho C_\phi = 0 \tag{4}$$

where $(')$ is the operator $d/d\theta$.

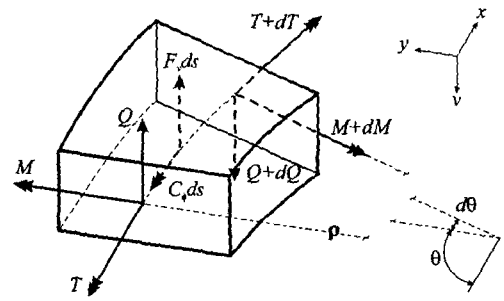

Fig. 2 Stress resultants and inertia forces

The equations that relate M and T to the rotation ψ and the torsional angle ϕ are[11]

$$M = EI\rho^{-1}(\phi - \psi') \tag{5}$$
$$T = GJ\rho^{-1}(\phi' - \psi) \tag{6}$$

where EI and GJ are flexural rigidity and torsional rigidity, respectively.

The horizontally curved beam is assumed to be in harmonic motion, or each coordinate is proportional to $\sin(\omega_i t)$ where ω_i is the i th circular frequency and t is time. The inertia forces per unit arc length are then

$$F_v = -\gamma A \omega_i^2 v \tag{7}$$
$$C_\phi = -E_\phi \gamma I_p \omega_i^2 \phi \tag{8}$$

where γ is the mass density, A is the cross-sectional area, I_p is the polar moment of inertia of the cross-section, and the index E_ϕ in Eq. (8) is defined as follows.

$E_\phi = 1$, if C_ϕ is included. (9.1)
$E_\phi = 0$, if C_ϕ is excluded. (9.2)

When Eqs. (5) and (6) are differentiated once, the results are

$$M' = EI\rho^{-1}[(\phi' - \psi'') - \rho^{-1}\rho'(\phi - \psi')] \quad (10)$$

$$T' = GJ\rho^{-1}[(\psi' + \phi'') - \rho^{-1}\rho'(\psi + \phi')] \quad (11)$$

When Eqs. (6) and (10) are substituted into Eq. (3), then

$$\begin{aligned} Q &= EI\rho^{-2}[(\phi' - \psi'') - \rho^{-1}\rho'(\phi - \psi')] \\ &\quad + GJ\rho^{-2}(\phi' + \psi) \end{aligned} \quad (12)$$

The following equation is obtained by differentiating Eq. (12).

$$\begin{aligned} Q' &= EI\rho^{-2}[(\phi'' - \psi''') - 3\rho^{-1}\rho'(\phi' - \psi'') \\ &\quad - \rho^{-1}\rho''(\phi - \psi') + 3\rho^{-2}\rho'^2(\phi - \psi')] \\ &\quad + GJ\rho^{-2}[(\phi'' + \psi') - 2\rho^{-1}\rho'(\phi' + \psi)] \end{aligned} \quad (13)$$

From Fig. 1, it is seen that the inclination θ is related to the coordinate x as follows.

$$\begin{aligned} \theta &= \pi/2 - \tan^{-1}(dy/dx) \\ &= \pi/2 - \tan^{-1}[(\pi h/l)\cos(\pi x/l)] \end{aligned} \quad (14)$$

When Eq. (14) is differentiated, the result is

$$d\theta = \pi^2 h \sin(\pi x/l)[l^2 + \pi^2 h^2 \cos^2(\pi x/l)]^{-1} dx \quad (15)$$

Define the following beam parameters.

$$g_1 = [\pi^{-2}h^{-1}l^2 + h\cos^2(\pi x/l)]\csc(\pi x/l) \quad (16.1)$$

$$g_2 = \frac{dg_1}{dx} \quad (16.2)$$

$$g_3 = \frac{d^2 g_1}{dx^2} \quad (16.3)$$

From Eq. (15), and with Eqs. (16.1) - (16.3), the following differential operators are obtained.

$$\frac{d}{d\theta} = g_1 \frac{d}{dx} \quad (17)$$

$$\frac{d^2}{d\theta^2} = {g_1}^2 \frac{d^2}{dx^2} + g_1 g_2 \frac{d}{dx} \quad (18)$$

$$\begin{aligned} \frac{d^3}{d\theta^3} &= {g_1}^3 \frac{d^3}{dx^3} + {g_1}^2 g_2 \frac{d^2}{dx^2} \\ &\quad + ({g_1}^2 g_3 + g_1 {g_2}^2)\frac{d}{dx} \end{aligned} \quad (19)$$

The radius of curvature ρ at any point of the sinusoidal curved beam is expressed as Eq. (20). Also, its derivatives ρ' and ρ'' can be expressed in terms of x by using Eq. (20) with Eqs. (17) and (18) as Eqs. (21) and (22), respectively. That is,

$$\begin{aligned} \rho &= [1 + (dy/dx)^2]^{3/2}(d^2y/dx^2)^{-1} \\ &= -[\pi^{-2}h^{-1}l^2 + h\cos^2(\pi x/l)]^{3/2}\csc(\pi x/l) \end{aligned} \quad (20)$$

$$\rho' = \frac{d\rho}{d\theta} = g_1 \frac{d\rho}{dx} \quad (21)$$

$$\rho'' = \frac{d^2\rho}{d\theta^2} = {g_1}^2 \frac{d^2\rho}{dx^2} + g_1 g_2 \frac{d\rho}{dx} \quad (22)$$

The following non-dimensional parameters are introduced.

$$s_p = l/\sqrt{I_p/A} \quad (23)$$

$$\varepsilon = GJ/(EI) \quad (24)$$

Here s_p and ε are the slenderness ratio about I_p and the stiffness parameter, respectively.

When Eqs. (7), (13), and (20)-(22) together with Eqs. (17)-(19) and (23) and (24) are used in Eq. (2), the result is Eq. (25). And when Eqs. (5), (8), (11) and (20)-(22) together with Eqs. (17)-(19) and (23) and (24) are used in Eq. (4), the result is Eq. (26). That is,

$$\begin{aligned} \psi^{iii} &= a_1\psi^{ii} + a_2\psi^{i} + a_3\psi + a_4\phi^{ii} + a_5\phi^{i} \\ &\quad + a_6\phi + {\omega_i}^2 a_7\delta \end{aligned} \quad (25)$$

$$\phi^{ii} = a_8\psi^{i} + a_9\psi + a_{10}\phi^{i} + (a_{11} + E_\phi {\omega_i}^2 a_{12})\phi \quad (26)$$

Finally the relationship between the vertical displacement v and the rotation of cross-section ψ is expressed as $dv/ds \approx dv/(\rho d\theta) = v'/\rho = \psi$ where ds is the arc length of small element in Fig. 2, and then this relation can be converted by using Eqs. (17) And (20) as

$$v^{i} = a_{13}\psi \quad (27)$$

In these latter three equations $(^{i})$ is the operator d/dx, and the constants are as follows.

$$a_1 = -{g_1}^{-1}(g_2 + 3b_1) \quad (28.1)$$

$$a_2 = {g_1}^{-2}(\varepsilon - g_1 g_3 - {g_2}^2 - 3g_2 b_1 - b_2 - 3{b_1}^2) \quad (28.2)$$

$$a_3 = 2\varepsilon\, {g_1}^{-3} b_1 \quad (28.3)$$

$$a_4 = (\varepsilon + 1){g_1}^{-1} \quad (28.4)$$

$$a_5 = g_1^{-2}(g_2 + \varepsilon g_2 + 5b_1) \quad (28.5)$$

$$a_6 = g_1^{-3}(3b_1^2 + b_2) \quad (28.6)$$

$$a_7 = \rho^3 g_1^{-3}(\gamma A / EI) \quad (28.7)$$

$$a_8 = (1+\varepsilon^{-1})g_1^{-1} \quad (28.8)$$

$$a_9 = g_1^{-2} b_1 \quad (28.9)$$

$$a_{10} = -g_1^{-1}(g_2 - b_1) \quad (28.10)$$

$$a_{11} = \varepsilon^{-1} g_1^{-2} \quad (28.11)$$

$$a_{12} = -\rho^2 g_1^{-2} \varepsilon^{-1} s_p^{-2} l^2 (\gamma A / EI) \quad (28.12)$$

$$a_{13} = \rho g_1^{-1} \quad (28.13)$$

where,

$$b_1 = -\rho^{-1}\rho^{i} \quad (29.1)$$

$$b_2 = -\rho^{-1}\rho^{ii} \quad (29.2)$$

Now consider the boundary conditions. At a clamped end ($x=0$ or $x=L$), the boundary conditions are $v=\psi=\phi=0$ and these relations can be expressed in the non-dimensional form as

$$v=0 \text{ at } x=0 \text{ or } x=L \quad (30)$$

$$\psi=0 \text{ at } x=0 \text{ or } x=L \quad (31)$$

$$\phi=0 \text{ at } x=0 \text{ or } x=L \quad (32)$$

At a hinged end ($x=0$ or $x=L$), the boundary conditions are $v=M=\phi=0$ and these relations can be expressed in the non-dimensional form as

$$v=0 \text{ at } x=0 \text{ or } x=L \quad (33)$$

$$\psi^{i}=0 \text{ at } x=0 \text{ or } x=L \quad (34)$$

$$\phi=0 \text{ at } x=0 \text{ or } x=L \quad (35)$$

Here, the Eq. (34) implies that the bending moment M expressed in Eq. (5) is zero.

3. Numerical Methods and Discussion

Based on the above analysis, a general FORTRAN computer program was written to calculate the frequency parameters ω_i and the corresponding mode shapes $\psi=\psi_i(x)$, $\phi=\phi_i(x)$ and $v=v_i(x)$. The numerical methods described by Lee et al.[1] and Lee and Wilson[9] were used to solve the differential Eqs. (25), (26) and (27), subjected to the end constraint Eqs. (30)-(32) or Eqs. (33)-(35). First, the Determinant Search method combined with the Regula-Falsi method was used to obtain the frequency parameter ω_i, and then the Runge-Kutta method was used to calculate the mode shapes ψ, ϕ and v.

Prior to execute the numerical studies, the convergence analysis, for which $f(=h/l)=0.2$, $e(=L/l)=0.7$, $s_p=50$, $\varepsilon=0.25$ and $E_\phi=1$, was conducted to determine the appropriate step size $\Delta\xi$ in the Runge-Kutta method, in which ξ is defined as x/l. Figure 3 shows $1/\Delta\xi$ versus $c_i(=\omega_i l^2\sqrt{\gamma A/EI})$ curves, in which a step size of $1/\Delta\xi=20$ is found to give convergence for c_i to within three significant figures. It is noted that the convergent efficiency herein is highly promoted, under same convergence criteria, comparing the $1/\Delta\xi=50$ obtained in polar coordinates by Mo[11]. However, the step size of $\Delta\xi=1/50$ was used herein in order to increase accuracy of numerical solutions.

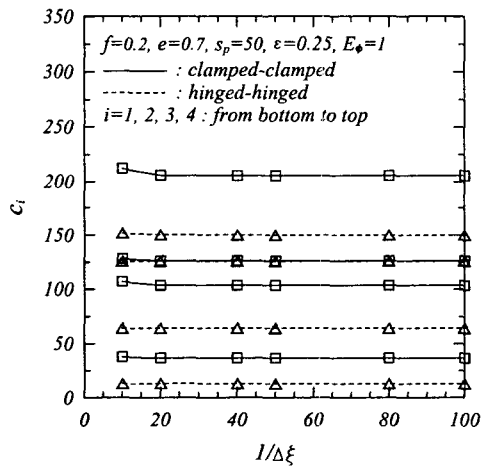

Fig. 3 Convergence analysis

Four lowest values of $c_i(i=1,2,3,4)$ and the corresponding mode shapes were calculated in this study. Numerical results, given in Table 1, Table 2 and Figs. 4 through 6, are now discussed.

The first series of numerical results are shown in Table 1. These studies served as an approximate check on the analysis presented herein. For comparative purposes, finite element solutions based on the commercial packages SAP 2000 were used to compute the first four frequency parameters c_i for two end constraints. The results showed that 100 three-dimensional finite frame elements were necessary to match within a tolerance of about 3% values of c_i computed by solving the governing

differential equations. It can be concluded that the present study gives accurate results.

Table 1 Comparisons of c_i between this study and SAP 2000

Geometry	i	Frq. parameter, c_i		Ratio*
		This study	SAP 2000	
Both clamped ends, $f=0.2$, $e=0.7$, $s_p=50$, $\varepsilon=0.25$, $E_\phi=1$	1	36.04	36.25	0.994
	2	101.5	102.4	0.991
	3	123.5	127.6	0.968
	4	201.3	201.7	0.998
Both hinged ends, $f=0.2$, $e=0.7$, $s_p=50$, $\varepsilon=0.25$, $E_\phi=1$	1	12.74	12.93	0.985
	2	62.83	63.67	0.987
	3	123.2	124.6	0.989
	4	146,2	149.1	0.980

* Ratio=(This study)/(SAP 2000)

All of numerical results that follow are based on the analysis reported herein. In Table 2, the effects of torsional inertia on natural frequencies are shown. It is apparent that the effect of torsional inertia is to always depress the natural frequencies, in which these depressions are less than about 1 %. Further, the frequencies of both clamped ends are always greater than those of both hinged ends, other parameters remaining the same.

Table 2 The effect of torsional inertia on frequency

Geometry	i	Frq. parameter, c_i		Ratio*
		$E_\phi=0$	$E_\phi=1$	
Both clamped ends, $f=0.3$, $e=0.75$, $s_p=80$, $\varepsilon=0.25$	1	25.75	25.68	0.997
	2	74.02	73.69	0.996
	3	150.7	149.9	0.995
	4	203.0	201.7	0.994
Both hinged ends, $f=0.3$, $e=0.75$, $s_p=80$, $\varepsilon=0.25$	1	7.23	7.16	0.990
	2	43.93	43.75	0.996
	3	107.8	107.1	0.994
	4	197.8	196.1	0.991

* Ratio=$(E_\phi=1)/(E_\phi=0)$

It is shown in Fig. 4, for which $e=0.75$, $s_p=50$, $\varepsilon=0.25$ and $E_\phi=1$, that each frequency curve of third modes of both clamped ends and both hinged ends reaches a peak as the horizontal rise to chord length ratio f is increased while the other frequency parameters decrease as f is increased. Further, it is observed for these unsymmetric curved beam configurations that two mode shapes can exist at a single frequency, a phenomena that was previously observed only for symmetric vertically curved beam i.e. arch configurations[10]. For both clamped ends, the second and third modes have the same frequencies $c_2=c_3=105.8$ at $f=0.061$ (marked as ■). However, the frequency curves of second and third modes for both hinged ends come close each other but not cross.

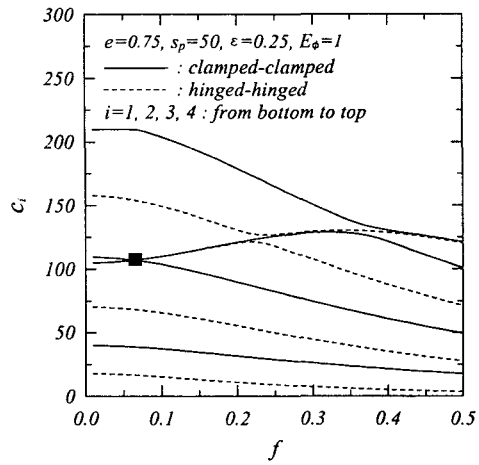

Fig. 4 c_i versus f curves

It is shown in Fig. 5, for which $f=0.2$, $s_p=50$, $\varepsilon=0.25$ and $E_\phi=1$, that the frequency parameters c_i decrease as the span length to chord length ratio e is increased. Particularly, it is noted that the frequency parameters of third and fourth mode are more significantly decreased as e gets smaller values.

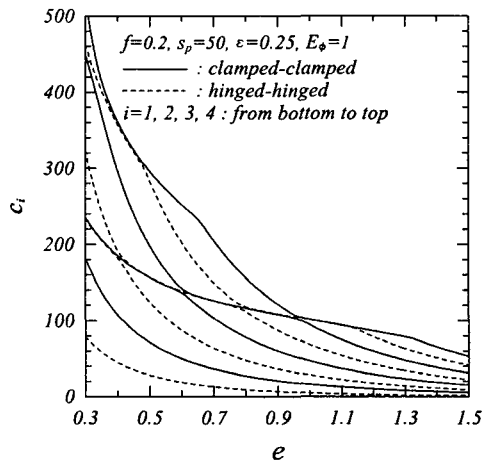

Fig. 5 c_i versus e curves

It is shown in Fig. 6, for which $f = 0.2$, $e = 0.75$, $\varepsilon = 0.25$ and $E_\phi = 1$, that the frequency parameters c_i increase, and in most cases approach a horizontal asymptote, as the slenderness ratio s_p is increased. It is noted that two pairs of lines cross, which shows that two mode shapes may exist at the same frequency as already shown in Fig. 4. That is, two modes of second and third modes for both clamped ends may exist where $c_2 = c_3 = 34.7$ at $s_p = 9.2$ (marked as ■).

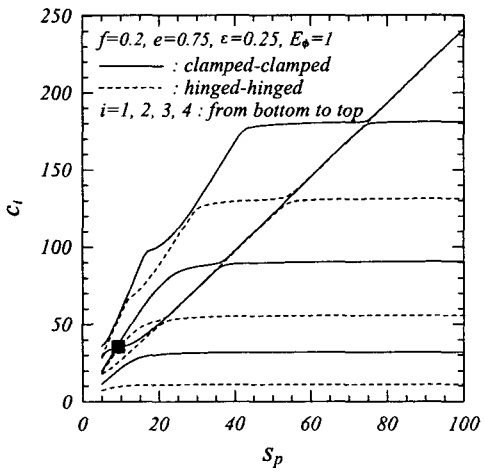

Fig. 6 c_i versus s_p curves

4. Concluding Remarks

This study deals with the free vibrations of the horizontally curved beams with unsymmetric axis. The governing differential equations are derived in Cartesian coordinates rather than in polar coordinates, in which the effect of torsional inertia on the natural frequencies is included. Differential equations, subjected to the sinusoidal curved beams, newly derived herein were solved numerically to calculate both natural frequencies and mode shapes. For validating the theories and numerical methods presented herein, frequency parameters obtained in this study are compared to those of SAP 2000. The convergence efficiency of the numerical methods developed herein is highly improved under the differential equations in Cartesian coordinates. As the numerical results, the relationships between the frequency parameters and the various non-dimensional beam parameters are reported, and typical mode shapes are presented. It is expected that results obtained herein can be practically utilized in the fields of vibration controls.

References

1. Lee, B.K., Oh, S.J. and Park. K.K., "Free vibrations of shear deformable circular curved beams resting on elastic foundation," International Journal of Structural Stability and Dynamics, Vol. 2, No. 1, 2002, pp.77-97.
2. Volterra, E. and Morell, J.D., "A note on the lowest natural frequency of elastic arcs," Journal of Applied Mechanics, Vol. 27, 1960, pp.744-746.
3. Romanelli, E. and Laura, P.A.A., "Fundamental frequency of non-circular, elastic, hinged arcs," Journal of Sound and Vibration, Vol. 24, No. 1, 1972, pp.17-22.
4. Maurizi, M.J., Rossi, R.E. and Belles, P.M., "Lowest natural frequency of clamped circular arcs of linearly tapered width," Journal of Sound and Vibration, Vol. 144, No. 3, 1991, pp.357-361.
5. Irie, T., Yamada G. and Tanaka, K., "Natural frequencies of out-of-plane vibration of arcs," Journal of Applied Mechanics, ASME, Vol. 49, 1982, pp.910-9137.
6. Kawakami, M., Sakiyama, T., Matsuda, H. and Morita, C., "In-plane and out-of-plane free vibrations of curved beams with variable sections," Journal of Sound and Vibration, Vol. 187, No. 3, 1995, pp.381-401.
7. Kang, K, Bert, C.W. and Striz, A.G., "Vibration analyses of horizontally curved beams with warping using DQM." Journal of Structural Engineering, ASCE, Vol. 122, No. 6, 1986, pp.657-662.
8. Yildirim, V., "A computer program for the free vibration analysis of elastic arcs," Computers & Structures, Vol. 62, No. 3, 1997, pp.475-485.
9. Lee, B.K. and Wilson, J.F., "Free vibrations of arches with variable curvature," Journal of Sound and Vibration, Vol.136, No. 1, 1989, pp.75-89.
10. Laskey, A.J., Out-of-plane vibrations of continuous circular curved beams considering shear deformation and rotatory inertia. M.S. Thesis, The University of New Hampshire, USA., 1981.
11. Mo, J.M., A study on free vibrations of horizontally curved beams with variable curvature. Ph.D. Thesis, Wonkwang University, Korea, 1997.